

## Accepted Manuscript

Design, synthesis, and biological activity of phenyl-pyrazole derivatives as BCR-ABL kinase inhibitors

Liming Hu, Yuyan Zheng, Zhipeng Li, Yujie Wang, Yongjuan Lv, Xuemei Qin, Chengchu Zeng

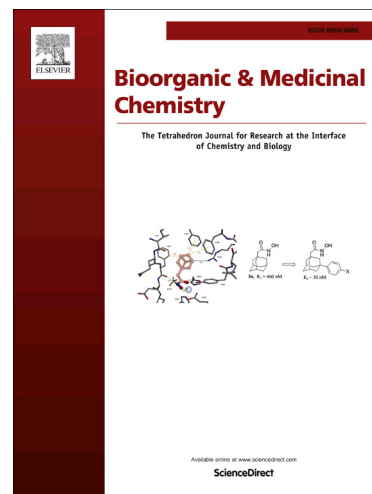
PII: S0968-0896(15)00404-6  
DOI: <http://dx.doi.org/10.1016/j.bmc.2015.04.083>  
Reference: BMC 12300

To appear in: *Bioorganic & Medicinal Chemistry*

Received Date: 9 February 2015  
Revised Date: 28 April 2015  
Accepted Date: 29 April 2015

Please cite this article as: Hu, L., Zheng, Y., Li, Z., Wang, Y., Lv, Y., Qin, X., Zeng, C., Design, synthesis, and biological activity of phenyl-pyrazole derivatives as BCR-ABL kinase inhibitors, *Bioorganic & Medicinal Chemistry* (2015), doi: <http://dx.doi.org/10.1016/j.bmc.2015.04.083>

This is a PDF file of an unedited manuscript that has been accepted for publication. As a service to our customers we are providing this early version of the manuscript. The manuscript will undergo copyediting, typesetting, and review of the resulting proof before it is published in its final form. Please note that during the production process errors may be discovered which could affect the content, and all legal disclaimers that apply to the journal pertain.





## Design, synthesis, and biological activity of phenyl-pyrazole derivatives as BCR-ABL kinase inhibitors

Liming Hu\*, Yuyan Zheng, Zhipeng Li, Yujie Wang, Yongjuan Lv, Xuemei Qin, Chengchu Zeng

College of Life Science and Bioengineering, Beijing University of Technology, Beijing 100124, China

### ARTICLE INFO

#### Article history:

Received  
 Received in revised form  
 Accepted  
 Available online

#### Keywords:

BCR-ABL  
 Tyrosine kinase inhibitor  
 Phenyl-pyrazole  
 Molecular docking

### ABSTRACT

4-(pyridin-3-yl)-1H-pyrazol-1-yl-phenyl-3-benzamide derivatives have been proposed as new BCR-ABL tyrosine kinase inhibitors by using combinational strategies of scaffold hopping and conformational constraint. In the present study, a series of 4-(pyridin-3-yl)-1H-pyrazol-1-yl-phenyl-3-benzamide derivatives were synthesized and their activities against BCR-ABL kinase in vitro were evaluated by using Kinase-Glo assay. All new compounds showed moderate to potent activities against wild-type (wt) BCR-ABL kinase with an IC<sub>50</sub> range from 14.2 to 326.0 nM. Among them, seven compounds exhibited BCR-ABL kinase inhibitory activities with IC<sub>50</sub> values less than 50nM. Compound **7a** displayed the most potent inhibitory activity to BCR-ABL kinase (IC<sub>50</sub>:14.2nM). Docking simulation was performed for compound **7a** and **7i** into the BCR-ABL kinase structure active site to determine the probable binding model. The preliminary structure-activity relationship was discussed. The interesting activities of these compounds may make them promising candidates as therapeutic agents for chronic myelogenous leukemia.

2015 Elsevier Ltd. All rights reserved.

### 1. Introduction

Chronic myeloid leukemia (CML) is clonal myeloproliferative disorder characterized by excessive proliferation of cells of the myeloid lineage and now represents about 20% of adult leukemia.<sup>1</sup> The occurrence of Philadelphia (Ph) chromosome is characteristic of CML and is caused by the reciprocal translocation involving chromosome 9 and chromosome 22. A segment of the c-ABL gene on chromosome 9q34 is transposed onto the BCR gene on chromosome 22q11, leading to the fusion of the Abelson tyrosine kinase (ABL) gene on chromosome 9 with the breakpoint cluster region (BCR) gene on chromosome 22 and the generation of a constitutively active chimeric BCR-ABL oncogene.<sup>2,3</sup> The encoded protein of the recombined gene is a fusion protein having constitutively active tyrosine kinase activity. The fusion protein BCR-ABL contains a GRB2 binding site, SH2 and SH3 domains, and a tyrosine-kinase(TK) domain and can activate several signaling pathways, such as the janus kinase(JAK)/signal transduction and transcription(STAT) pathway, phosphatidylinositol-3 (PI3) kinase pathway, RAS/mitogen-activated protein kinase (MAPK) pathways, and the myc pathway.<sup>4</sup> Since the BCR-ABL protein exists in greater than 90% of CML cases, it has become a well-validated and novel target for designing small molecular inhibitors to treat CML.<sup>5</sup>

Imatinib (STI571) approved by FDA in 2001, has been a great success for curing CML (Figure 1).<sup>6</sup> It is now treated as a first-line drug in conventional treatment of CML because of its high efficacy and lower side effects.<sup>7</sup> Surfacing resistance has become

a great challenge despite of the clear success of imatinib.<sup>8</sup> The main mechanism of resistance is the overexpression of BCR-ABL, mainly due to point mutations in the BCR-ABL kinase domain. Currently, more than 100 mutations have been discovered in patients with imatinib-resistant CML.<sup>5,9</sup>

To overcome resistances, several second-generation drugs have been designed and synthesized, including nilotinib (AMN107) and dasatinib (BMS-354825) to treat patients in all phases of CML with resistances to imatinib (Figure 1).<sup>10,11</sup> Most recently, some third-generation BCR-ABL tyrosine kinase inhibitors were disclosed to inhibit almost the full range of BCR-ABL kinase domain mutations as well as the native kinase. Ponatinib (AP24534) has been advanced for clinical investigation (Figure 1)<sup>5</sup>. Although second-generation drugs can inhibit some imatinib-resistant BCR-ABL mutants, there are still significant numbers of resistant mutants which no alternative drugs could overcome. Consequently, there is still necessary to discovery new compounds that will enrich the pool of known tyrosine kinase inhibitors.<sup>12</sup>

So far, several cocrystal structures of BCR-ABL kinase with their inhibitors have been reported. These inhibitors possessed some key structural elements which formed crucial interactions between the protein and inhibitors base on of structural analysis of the inhibitors (i.e., imatinib and ponatinib) and BCR-ABL kinase. There are four key structural elements: (1) "head region", a heterocyclic moiety which binds to the adenine pocket and forms a hydrogen bond network with residues in the hinge region; (2) "middle part", a methylphenyl group which occupies the hydrophobic pocket behind the gatekeeper residue; (3) "tail

Correspondence: huliming@bjut.edu.cn, Tel:+86 10 6739 6211

region”, an additional hydrophobic group which binds the pocket; (4) “linker part”, a moderate linker between the head region and the middle part to avoid the steric clash with the residue of BCR-ABL.<sup>1</sup> Basing on the analysis, a series of phenyl-pyrazole

derivatives **7** are designed as BCR-ABL kinase inhibitors in which a moderate pyrazole linker is utilized between the head region and the middle part ( a methylphenyl group) as shown in Figure 2.

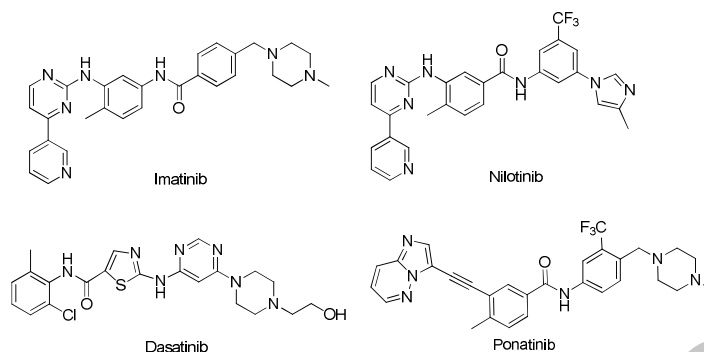


Figure1. Chemical structures of FDA-approved BCR-ABL inhibitors and newly developed Ponatinib.

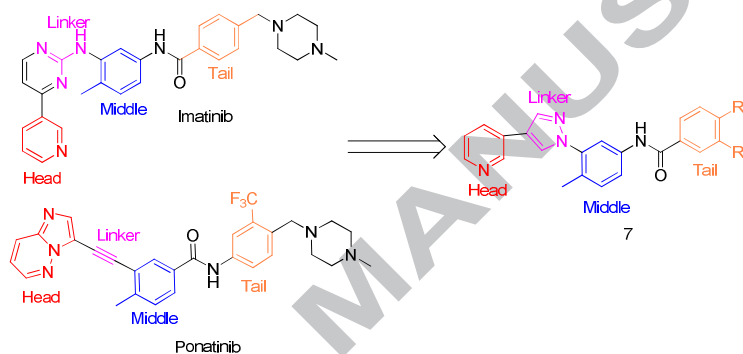


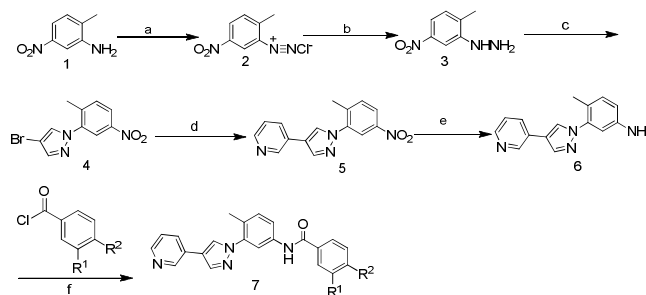
Figure 2. Design of phenyl-pyrazole derivative as new BCR-ABL inhibitor.

## 2. Results and discussion

### 2.1. Chemistry

The synthesis of target compounds **7a-7n** was outlined in Scheme 1. Compound **2** was produced by diazotization of aromatic amine 2-methyl-5-nitroaniline (**1**). 2-Methyl-5-nitrophenylhydrazine (**3**) was synthesized by reduction reaction of the intermediate **2** with stannous chloride dihydrate. 2-bromomalon-aldehyde was treated with **3** to produce 4-bromo-1-(2-methyl-5-nitrophenyl)-1H-pyrazole (**4**) by ring-closure reaction. The intermediate **4** reacted with 3-pyridylboronic acid to obtain 3-(1-(2-methyl-5-nitrophenyl)-1H-pyrazol-4-yl)pyridine (**5**) by Heck coupling reaction under nitrogen atmosphere. 4-methyl-3-

(pyridin-3-yl) aniline (**6**) was produced by reduction reaction of the intermediate **5** with hydrogen in the presence of Pd/C. Variable substituted benzoyl chloride in anhydrous dichloromethane was added dropwise to compound **6** at 0 °C in the presence of triethylamine and then the reaction mixture was slowly warmed to temperature and stirred 4-6 h till TLC confirmed that the reaction had finished. Then the mixture solutions were filtered to afford the target compounds **7a-7n**. The products were purified by recrystallization in EtOH to obtain **7a-7n**.



Scheme 1. Reactions and conditions: (a) NaNO<sub>2</sub>, HCl, H<sub>2</sub>O, 0-5 °C; (b) SnCl<sub>2</sub>·H<sub>2</sub>O, HCl, H<sub>2</sub>O, 0-5 °C, 70-75 %; (c) 2-bromomalon-aldehyde, EtOH, 80 °C, 2 h, 30-40 %; (d) 3-pyridylboronic acid, Pd(PPh<sub>3</sub>)<sub>4</sub>, Na<sub>2</sub>CO<sub>3</sub>, dioxane/H<sub>2</sub>O(3:1), 100 °C, 6 h, 70-75%; (e) H<sub>2</sub>, Pd/C, EtOH, rt; (f) triethylamine, CH<sub>2</sub>Cl<sub>2</sub>, 0 °C, rt, 4 h, 60-70 %.

## 2.2. Inhibition of BCR-ABL activity

Table 1 lists the structures of the tested compounds and their corresponding  $IC_{50}$  values. All new compounds showed moderate potent activities against wild-type (wt) BCR-ABL1 kinase with an  $IC_{50}$  range from 14.2 to 326.0 nM. Among them, seven compounds exhibited BCR-ABL1 kinase inhibitory activities with  $IC_{50}$  values less than 50 nM. Interestingly, **7a**, **7b**, **7m** exhibit an  $IC_{50}$  value as low as 14.2 nM, 15.9 nM, 16.8 nM in BCR-ABL kinase inhibition, about 10-fold lower than control compound Staurosporine (STSP) respectively. Compound **7a** stands out as the most active compound in the set with an  $IC_{50}$  value of 14.2 nM which clearly reveals that the large hydrophobic group is detrimental to the activities on tyrosine kinase and its physicochemical properties to keep ideal hydrophil-lipophilic balance of the molecules. This group was also widely found in the chemical structures of many other

kinase inhibitors. Moreover, compounds (**7d**, **7e**, **7f** and **7k**) was also about three times higher than that of control compound STSP. These results showed that these compounds were the novel BCR-ABL kinase inhibitors. Furthermore, antitumor activities of the compounds **7a-7n** were evaluated against BCR-ABL positive leukemia cell in comparison with control compound STSP. Not surprisingly, most compounds also displayed moderate suppression on the growth of the human chronic myelogenous leukaemia K562 cells expressing high level of BCR-ABL protein. In particular, compound **7a** potently inhibited the growth of K562 cells with an  $IC_{50}$  value of 0.27  $\mu$ M, which was about hundreds of times fold lower than that of control compound STSP (153  $\mu$ M). Besides, the antitumor activity of other compounds was higher than that of control STSP.

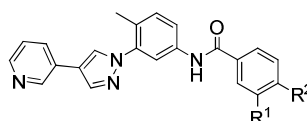


**Table 1.** Inhibitory activities of compounds **7a-7n** towards BCR-ABL kinase and K562 cells in vitro

Compd.	R <sup>1</sup>	R <sup>2</sup>	BCR-ABL Kinase	
			IC <sub>50</sub> (nM)	K562 Cells IC <sub>50</sub> (μM)
<b>7a</b>	3-CF <sub>3</sub>	H	14.20	0.27
<b>7b</b>	3-Cl	H	15.90	1.32
<b>7c</b>	H	4-F	213.5	12.49
<b>7d</b>	H	4-CH <sub>2</sub> CH <sub>3</sub>	41.02	6.52
<b>7e</b>	H	4-CF <sub>3</sub>	43.27	0.76
<b>7f</b>	H	4-OCH <sub>3</sub>	46.20	18.3
<b>7g</b>	H		50.60	1.67
<b>7h</b>	H		178.0	21.5
<b>7i</b>	H		326.0	136.0
<b>7j</b>	H		129.1	3.26
<b>7k</b>	H		26.58	8.65
<b>7l</b>	H		117.4	2.74
<b>7m</b>	H		16.87	2.33
<b>7n</b>	H		175.3	98.3
STSP			121.8	153.0

## 2.3. Docking Studies

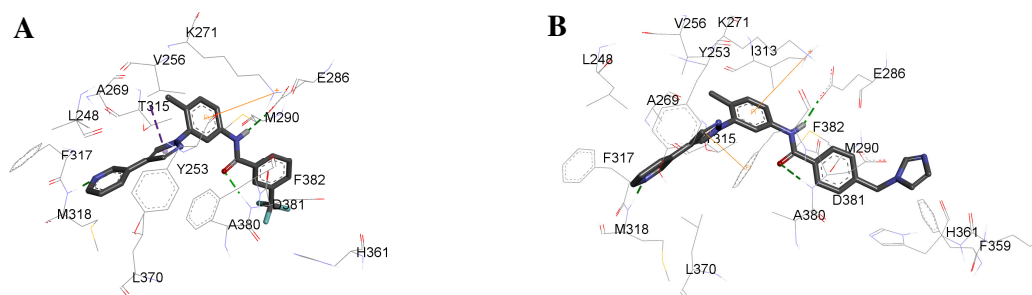


**Figure 3.** A and B show the binding model of inhibitor **7a** and **7i** to BCR-ABL kinase. Oxygen atom (red stick), nitrogen atom (blue stick), H-bond (green dash line), pi-pi stack (purple dash line).

To investigate the possible bonding mechanism of these compounds, compound **7a** and **7i** were selected for docking studies. The binding mode of selected molecule was studied by Autodock 4.0 with the help of AutodockTools. BCR-ABL tyrosine kinase (PDB:3cs9) was selected as the receptor for docking study. The best docking conformation was selected for the analysis and the docking result is shown in Figure 2. The pyridazine moiety in **7a** and **7i** could form an essential hydrogen bond with the NH of Met318 in the hinge region of Bcr-Abl. Moreover, the amide also formed two hydrogen bonds with Glu286 and Asp381. However, the pyrazole linker in **7a** could form pi-pi stacking interaction with Thr315 of BCR-ABL, which may cause that inhibitory activities of compound **7a** towards BCR-ABL kinase is stronger than compound **7i**.

### 3. Conclusion

In summary, a series of novel phenyl-pyrazole BCR-ABL tyrosine kinase inhibitors were synthesized and identified as BCR-ABL tyrosine kinase. The result indicates that compound **7a** exhibited an  $IC_{50}$  value as low as 14.2 nM and showed highly inhibition to BCR-ABL tyrosine kinase. **7a** may be proved as a new promising lead compound for the further development of new BCR-ABL inhibitors overcoming the clinical acquired resistance.

## 4. Experimental section

### 4.1. Chemistry

Unless otherwise noted, all materials were obtained from commercial suppliers and dried and purified by standard procedures. Melting points were determined on a Beijing Keyi elec-opti instrument factory melting point apparatus. Proton nuclear magnetic resonance ( $^1H$  NMR) spectra were recorded with a Bruker Avance DRX400 spectrometer with  $CDCl_3$  or  $DMSO-d_6$  as the solvent and tetramethyl-silane (TMS) as the internal standard. The chemical shifts were reported in  $\delta$  (ppm). Mass spectra (MS) data were obtained using Esquire6000 Mass Spectrometer. Petroleum ether used for column chromatography had a boiling range of 60-90  $^{\circ}C$ .<sup>13</sup>

#### 4.1.1. (2-methyl-5-nitrophenyl)hydrazine (**3**)

2-methyl-5-nitroaniline (3.0 g, 19.7 mmol) was dissolved in a mixture of  $H_2O$  (5 mL) and 37% HCl (5 mL). A solution of  $NaNO_2$  (1.4 g, 20.3 mmol) in  $H_2O$  (15 mL) was added dropwise at 0  $^{\circ}C$ , followed by the addition of  $SnCl_2 \cdot H_2O$  (9.0 g, 39.8 mmol) in 37% HCl (7 mL) at that temperature. After stirring at 0  $^{\circ}C$  for 0.5 h, the reaction mixture was neutralized with 1M NaOH to pH 7-8, and extracted with DCM. The organic phase was separated and dried over anhydrous  $MgSO_4$ . The organic phase was concentrated under reduced pressure and the residue

was purified by column chromatography (silica gel, petroleum ether:ethyl acetate = 4:1) to give the solid (2.3 g). Yellow solid; yield: 70.0%;  $^1H$  NMR ( $DMSO-d_6$ , 400 MHz,  $\delta$  ppm): 7.84 (d, J = 2.4 Hz, 1H), 7.37 (dd, J = 8.1, 2.4 Hz, 1H), 7.16 (d, J = 8.1 Hz, 1H), 6.88 (s, 1H), 4.22 (s, 2H), 2.13 (s, 3H). MS (ESI): m/z 168.1  $[M+H]^+$ .

#### 4.1.2. 4-bromo-1-(2-methyl-5-nitrophenyl)-1H-pyrazole (**4**)

2-bromomalonaldehyde (2.4 g, 16.0 mmol) in EtOH (15 mL) was treated with (2-methyl-5-nitrophenyl) hydrazine (4.0 g, 23.9 mmol) and refluxed for 1 h. The reaction mixture was concentrated under reduced pressure and the residue was purified by column chromatography (silica gel, petroleum ether:ethyl acetate=12:1) to the solid (1.4 g). Yellow solid; yield: 30%;  $^1H$  NMR ( $CDCl_3$ , 400 MHz,  $\delta$  ppm): 8.36-8.10 (m, 2H), 7.74 (d, J = 8.2 Hz, 2H), 7.53 (d, J = 8.7 Hz, 1H), 2.43 (s, 3H). MS (ESI): m/z 281.4  $[M+H]^+$ .

#### 4.1.3. 3-(1-(2-methyl-5-nitrophenyl)-1H-pyrazol-4-yl)pyridine (**5**)

The boronic acid (1.8 g, 14.6mmol), the arylhalide (2.0 g, 7.1 mmol) and  $Pd(PPh_3)_4$  (0.4 g, 0.35 mmol) were sequentially added to degassed 1,4-dioxane (10 mL) and the mixture was stirred at 25  $^{\circ}C$  for 10 min. Degassed aqueous  $Na_2CO_3$  solution (1 M, 14.2 mmol) was added and the reaction mixture was heated under argon at reflux for 6 h. The mixture was filtered and concentrated under reduced pressure and the residue was purified by column chromatography (silica gel, petroleum ether:ethyl acetate = 1:1) to give the solid (1.5 g). Light yellow solid; yield: 72%;  $^1H$  NMR ( $CDCl_3$ , 400 MHz,  $\delta$  ppm): 8.87 (s, 1H), 8.56 (d, J = 3.9 Hz, 1H), 8.31 (d, J = 2.2 Hz, 1H), 8.24 (dd, J = 8.5, 2.2 Hz, 1H), 8.10 (s, 1H), 8.00 (s, 1H), 7.87 (d, J = 7.9 Hz, 1H), 7.57 (d, J = 8.4 Hz, 1H), 7.28 (s, 1H), 2.06 (s, 3H). MS (ESI): m/z: 281.1  $[M+H]^+$ .

#### 4.1.4. 4-methyl-3-(4-(pyridin-3-yl)-1H-pyrazol-1-yl)aniline (**6**)

Compounds **5** (1.0 g, 3.6 mmol) in EtOH (10 mL) was hydrogenated over Pd/C (0.1 g) under balloon pressure over night. The mixture was filtered and the filtrate was under reduced pressure to the next step directly.

#### 4.1.5. General procedure for the synthesis of derivatives 7.

The appropriate Benzoyl chloride (1.2 mmol) in  $CH_2Cl_2$  (10 mL) was added to an ice cooled solution of compound **6** (1.2 mmol),  $Et_3N$  (0.2 mL), and  $CH_2Cl_2$  (5 mL). The solution was allowed to stir at room temperature for 3 h. A large amount of solid precipitated and was filtered. The residue was purified by recrystallization in EtOH.

##### 4.1.5.1 N-(4-methyl-3-(4-(pyridin-3-yl)-1H-pyrazol-1-yl)phenyl)-3-(trifluoromethyl)benzamide (**7a**)

White solid; yield: 65.0%; m.p. 178-179 °C; <sup>1</sup>H NMR (DMSO-*d*<sub>6</sub>, 400 MHz, δ ppm): 10.68 (s, 1H), 9.02 (s, 1H), 8.71 (s, 1H), 8.48 (d, J = 4.1 Hz, 1H), 8.43-8.23 (m, 3H), 8.16 (t, J = 17.2 Hz, 1H), 7.97 (d, J = 10.7 Hz, 2H), 7.80 (dd, J = 15.3, 7.9 Hz, 2H), 7.48 (dt, J = 12.1, 6.0 Hz, 1H), 7.42 (d, J = 8.4 Hz, 1H), 2.27 (s, 3H). <sup>13</sup>C NMR (DMSO-*d*<sub>6</sub>, 100 MHz, δ ppm): 164.52, 147.04, 146.16, 139.76, 138.46, 137.92, 135.94, 133.67, 132.33, 131.91, 130.23, 129.86, 129.54, 129.44, 128.90, 128.73, 128.72, 128.29, 124.66, 120.75, 119.90, 118.16, 17.93. HRMS (ESI): m/z 423.1433 calcd for C<sub>23</sub>H<sub>17</sub>F<sub>3</sub>N<sub>4</sub>O [M+H]<sup>+</sup>, found 423.1432.

#### 4.1.5.2 3-chloro-N-(4-methyl-3-(4-(pyridin-3-yl)-1H-pyrazol-1-yl)phenyl)benzamide (7b)

White solid; yield: 70.0%; m.p. 160-164 °C; <sup>1</sup>H NMR (DMSO-*d*<sub>6</sub>, 400 MHz, δ ppm): 10.50 (s, 1H), 8.99 (s, 1H), 8.68 (s, 1H), 8.45 (d, J = 4.7 Hz, 1H), 8.32 (s, 1H), 8.10 (d, J = 7.9 Hz, 1H), 8.03 (s, 1H), 7.99-7.90 (m, 2H), 7.79 (d, J = 8.3 Hz, 1H), 7.67 (d, J = 7.9 Hz, 1H), 7.58 (t, J = 7.9 Hz, 1H), 7.42 (t, J = 6.7 Hz, 2H), 2.26 (s, 3H). <sup>13</sup>C NMR (DMSO-*d*<sub>6</sub>, 100 MHz, δ ppm): 164.55, 147.88, 147.02, 139.80, 138.38, 137.97, 137.07, 133.74, 132.80, 131.98, 131.89, 130.90, 129.25, 128.51, 128.20, 127.85, 126.94, 124.31, 120.58, 120.17, 118.03, 17.93. HRMS (ESI): m/z 389.1169 calcd for C<sub>22</sub>H<sub>17</sub>ClN<sub>4</sub>O [M+H]<sup>+</sup>, found 389.1167.

#### 4.1.5.3 4-fluoro-N-(4-methyl-3-(4-(pyridin-3-yl)-1H-pyrazol-1-yl)phenyl)benzamide (7c)

White solid; yield: 75.0%; m.p. 186-190 °C; <sup>1</sup>H NMR (DMSO-*d*<sub>6</sub>, 400 MHz, δ ppm): 10.51 (s, 1H), 9.13 (s, 1H), 8.79 (s, 1H), 8.57 (d, J = 4.8 Hz, 1H), 8.50-8.30 (m, 2H), 8.08 (dt, J = 18.1, 9.0 Hz, 2H), 8.02 (d, J = 1.6 Hz, 1H), 7.79 (dd, J = 8.3, 1.7 Hz, 1H), 7.68 (dd, J = 7.9, 5.2 Hz, 1H), 7.38 (dd, J = 17.8, 8.8 Hz, 3H), 2.26 (s, 3H). <sup>13</sup>C NMR (DMSO-*d*<sub>6</sub>, 100 MHz, δ ppm): 164.96, 144.48, 143.58, 139.61, 138.63, 138.23, 136.22, 131.85, 131.51, 131.49, 130.96, 130.87, 130.10, 129.98, 127.95, 125.69, 120.74, 119.09, 117.98, 115.92, 115.71, 17.89. HRMS (ESI): m/z 373.1465 calcd for C<sub>22</sub>H<sub>17</sub>FN<sub>4</sub>O [M+H]<sup>+</sup>, found 373.1462.

#### 4.1.5.4 4-fluoro-N-(4-methyl-3-(4-(pyridin-3-yl)-1H-pyrazol-1-yl)phenyl)benzamide (7d)

White solid; yield: 76.0%; m.p. 186-190 °C; <sup>1</sup>H NMR (DMSO-*d*<sub>6</sub>, 400 MHz, δ ppm): 10.34 (s, 1H), 8.99 (s, 1H), 8.68 (s, 1H), 8.44 (d, J = 3.8 Hz, 1H), 8.31 (s, 1H), 8.10 (d, J = 7.8 Hz, 1H), 7.99 (s, 1H), 7.91 (d, J = 8.0 Hz, 2H), 7.72 (ddd, J = 18.1, 17.3, 5.9 Hz, 3H), 7.45-7.32 (m, 4H), 3.35 (s, 3H), 2.50 (s, 2H), 2.23 (t, J = 20.4 Hz, 3H). <sup>13</sup>C NMR (DMSO-*d*<sub>6</sub>, 100 MHz, δ ppm): 165.93, 148.35, 147.85, 146.99, 139.75, 138.34, 132.78, 132.55, 132.18, 132.09, 131.96, 131.80, 129.25, 129.12, 128.53, 128.25, 127.75, 124.32, 120.45, 120.10, 117.86, 28.54, 19.11, 17.91. HRMS (ESI): m/z 383.1872 calcd for C<sub>24</sub>H<sub>22</sub>N<sub>4</sub>O<sub>2</sub> [M+H]<sup>+</sup>, found 383.1869.

#### 4.1.5.5 N-(4-methyl-3-(4-(pyridin-3-yl)-1H-pyrazol-1-yl)phenyl)-4-(trifluoromethyl)benzamide (7e)

White solid; yield: 68.0%; m.p. 225-226 °C; <sup>1</sup>H NMR (DMSO-*d*<sub>6</sub>, 400 MHz, δ ppm): 10.64 (s, 1H), 8.99 (d, J = 1.7 Hz, 1H), 8.69 (s, 1H), 8.45 (dd, J = 4.7, 1.4 Hz, 1H), 8.33 (s, 1H), 8.16 (t, J = 10.6 Hz, 2H), 8.13-8.06 (m, 1H), 7.98 (t, J = 5.9 Hz, 1H), 7.93 (d, J = 8.3 Hz, 2H), 7.79 (dd, J = 8.3, 2.0 Hz, 1H), 7.42 (dd, J = 6.3, 2.3 Hz, 2H), 2.27 (s, 3H). <sup>13</sup>C NMR (DMSO-*d*<sub>6</sub>, 100 MHz, δ ppm): 164.88, 147.87, 147.00, 139.81, 138.89, 138.40, 137.91, 132.79, 131.94, 129.27, 129.05, 128.50, 128.50, 128.30, 128.30, 125.92, 125.89, 125.72, 124.32, 120.59, 120.17, 118.02, 17.95. HRMS (ESI): m/z 423.1433 calcd for C<sub>23</sub>H<sub>17</sub>F<sub>3</sub>N<sub>4</sub>O [M+H]<sup>+</sup>, found 423.1425.

#### 4.1.5.6 4-methoxy-N-(4-methyl-3-(4-(pyridin-3-yl)-1H-pyrazol-

#### 1-yl)phenyl)benzamide (7f)

White solid; yield: 70.0%; m.p. 208-209 °C; <sup>1</sup>H NMR (DMSO-*d*<sub>6</sub>, 400 MHz, δ ppm): 10.25 (s, 1H), 8.99 (d, J = 1.9 Hz, 1H), 8.67 (s, 1H), 8.45 (d, J = 4.6 Hz, 1H), 8.31 (s, 1H), 8.10 (d, J = 7.9 Hz, 1H), 8.02-7.91 (m, 3H), 7.78 (dt, J = 11.7, 5.8 Hz, 1H), 7.50-7.32 (m, 2H), 7.07 (d, J = 8.7 Hz, 2H), 3.84 (s, 3H), 2.25 (s, 3H). <sup>13</sup>C NMR (DMSO-*d*<sub>6</sub>, 100 MHz, δ ppm): 165.41, 162.50, 147.85, 147.00, 139.76, 138.47, 138.31, 132.79, 131.76, 130.05, 129.24, 129.11, 128.54, 127.63, 127.16, 127.16, 124.31, 120.47, 120.11, 117.90, 114.13, 55.91, 17.87. HRMS (ESI): m/z 385.1665 calcd for C<sub>23</sub>H<sub>20</sub>N<sub>4</sub>O<sub>2</sub> [M+H]<sup>+</sup>, found 385.1667.

#### 4.1.5.7 N-(4-methyl-3-(4-(pyridin-3-yl)-1H-pyrazol-1-yl)phenyl)-4-((4-methylpiperazin-1-yl)methyl)benzamide (7g)

Light yellow solid; yield: 80.0%; m.p. 209-211 °C; <sup>1</sup>H NMR (DMSO-*d*<sub>6</sub>, 400 MHz, δ ppm): 10.32 (d, J = 48.9 Hz, 1H), 8.94 (d, J = 36.3 Hz, 1H), 8.69 (s, 1H), 8.44 (d, J = 4.6 Hz, 1H), 8.32 (s, 1H), 8.10 (d, J = 7.9 Hz, 1H), 7.98 (d, J = 1.8 Hz, 1H), 7.92 (d, J = 8.1 Hz, 2H), 7.81-7.66 (m, 2H), 7.48-7.41 (m, 2H), 3.82 (s, 2H), 3.36 (s, 8H), 2.50 (s, 3H), 2.25 (s, 3H). <sup>13</sup>C NMR (CDCl<sub>3</sub>, 100 MHz, δ ppm): 165.78, 147.76, 146.94, 142.69, 139.57, 137.83, 136.80, 133.33, 132.82, 131.77, 129.28, 129.20, 128.29, 127.71, 127.22, 123.78, 120.55, 120.25, 118.07, 62.41, 54.95, 52.87, 45.84, 17.75. HRMS (ESI): m/z 467.2559 calcd for C<sub>28</sub>H<sub>30</sub>N<sub>6</sub>O [M+H]<sup>+</sup>, found 467.2556.

#### 4.1.5.8 4-methoxy-N-(4-methyl-3-(4-(pyridin-3-yl)-1H-pyrazol-1-yl)phenyl)benzamide (7h)

White solid; yield: 82.0%; m.p. 197-199 °C; <sup>1</sup>H NMR (CDCl<sub>3</sub>, 400 MHz, δ ppm): 8.79 (s, 1H), 8.63 (s, 1H), 8.47 (s, 1H), 7.96 (d, J = 17.9 Hz, 1H), 7.91 (s, 1H), 7.88-7.76 (m, 4H), 7.55 (d, J = 8.1 Hz, 1H), 7.41 (d, J = 7.8 Hz, 2H), 7.35-7.20 (m, 2H), 3.67 (t, J = 21.6 Hz, 4H), 3.55 (s, 2H), 2.45 (s, 4H), 2.24 (s, 3H); <sup>13</sup>C NMR (CDCl<sub>3</sub>, 100 MHz, δ ppm): 165.77, 147.64, 146.82, 141.91, 139.55, 137.84, 136.77, 133.56, 132.90, 131.76, 129.36, 129.24, 127.72, 127.27, 123.83, 120.60, 120.23, 118.13, 66.79, 62.78, 53.52, 17.70. HRMS (ESI): m/z 454.2243 calcd for C<sub>27</sub>H<sub>27</sub>N<sub>2</sub>O<sub>2</sub> [M+H]<sup>+</sup>, found 454.2243.

#### 4.1.5.9 4-((1H-imidazol-1-yl)methyl)-N-(4-methyl-3-(4-(pyridin-3-yl)-1H-pyrazol-1-yl)phenyl)benzamide (7i)

White solid; yield: 75.0%; m.p. 162-164 °C; <sup>1</sup>H NMR (CDCl<sub>3</sub>, 400 MHz, δ ppm): 8.84 (s, 1H), 8.58-8.45 (m, 2H), 8.02 (s, 1H), 7.96 (s, 1H), 7.87 (dd, J = 19.8, 8.2 Hz, 4H), 7.61 (dd, J = 13.6, 5.2 Hz, 2H), 7.34 (dd, J = 11.8, 6.6 Hz, 2H), 7.23 (d, J = 8.0 Hz, 2H), 7.13 (s, 1H), 6.94 (s, 1H), 5.21 (s, 2H), 2.31 (s, 3H). <sup>13</sup>C NMR (DMSO-*d*<sub>6</sub>, 100 MHz, δ ppm): 165.69 (s), 147.86 (s), 146.98 (s), 141.76 (s), 139.75 (s), 138.36 (s), 138.30 (s), 138.21 (s), 137.97 (s), 134.54 (s), 132.80 (s), 131.85 (s), 129.27 (s), 128.76 (s), 128.58 (s), 128.54 (s), 127.91 (s), 124.34 (s), 120.50 (s), 120.37 (s), 120.29 (s), 120.12 (s), 117.89 (s), 101.10 (s), 49.70 (s), 17.93 (s). HRMS (ESI): m/z 435.1933 calcd for C<sub>26</sub>H<sub>22</sub>N<sub>6</sub>O [M+H]<sup>+</sup>, found 435.1935.

#### 4.1.5.10 4-((diethylamino)methyl)-N-(4-methyl-3-(4-(pyridin-3-yl)-1H-pyrazol-1-yl)phenyl)benzamide (7j)

White solid; yield: 80.0%; m.p. 169-172 °C; <sup>1</sup>H NMR (CDCl<sub>3</sub>, 400 MHz, δ ppm): 8.81 (t, J = 11.5 Hz, 1H), 8.49 (dt, J = 13.3, 6.6 Hz, 1H), 8.01 (s, 2H), 7.95 (s, 1H), 7.85-7.78 (m, 4H), 7.57 (dd, J = 8.3, 2.3 Hz, 1H), 7.48 (d, J = 8.1 Hz, 2H), 7.32 (dd, J = 8.2, 4.2 Hz, 2H), 2.63-2.48 (m, 4H), 2.29 (s, 3H), 1.06 (t, J = 7.1 Hz, 6H); <sup>13</sup>C NMR (CDCl<sub>3</sub>, 100 MHz, δ ppm): 165.94, 147.73, 146.93, 144.19, 139.53, 137.80, 136.87, 133.12, 132.81, 131.72, 129.17, 129.05, 128.31, 127.72, 127.19, 123.76, 120.64,

120.23, 118.14, 57.20, 46.87, 17.68, 11.61. HRMS (ESI): *m/z* 440.2450 calcd for  $C_{27}H_{29}N_5O$  [M+H]<sup>+</sup>, found 440.2451.

4.1.5.11 4-((4-methyl-1,4-diazepan-1-yl)methyl)-N-(4-methyl-3-(4-(pyridin-3-yl)-1H-pyrazol-1-yl)phenyl)benzamide (**7k**)

White solid; yield: 79.0%; m.p. 178-180 °C; <sup>1</sup>H NMR (CDCl<sub>3</sub>, 400 MHz, δ ppm): 8.78 (d, *J* = 1.7 Hz, 1H), 8.74 (s, 1H), 8.46 (dd, *J* = 4.8, 1.4 Hz, 1H), 7.97 (s, 1H), 7.91 (s, 1H), 7.87-7.76 (m, 4H), 7.56 (dd, *J* = 8.3, 2.0 Hz, 1H), 7.40 (d, *J* = 8.1 Hz, 2H), 7.34-7.26 (m, 1H), 7.24 (d, *J* = 8.4 Hz, 1H), 3.64 (s, 2H), 2.72-2.63 (m, 6H), 2.60 (d, *J* = 5.7 Hz, 2H), 2.36 (s, 3H), 2.23 (s, 3H), 1.89-1.72 (m, 2H). <sup>13</sup>C NMR (CDCl<sub>3</sub>, 100 MHz, δ ppm): 165.95, 147.73, 146.92, 144.05, 139.52, 137.80, 136.88, 133.19, 132.80, 131.73, 129.14, 128.91, 128.29, 127.73, 127.24, 123.78, 120.62, 120.21, 118.13, 62.38, 57.34, 56.62, 54.31, 46.86, 27.27, 17.72. HRMS (ESI): *m/z* 481.2716 calcd for  $C_{29}H_{32}N_6O$  [M+H]<sup>+</sup>, found 481.2716.

4.1.5.12 N-(4-methyl-3-(4-(pyridin-3-yl)-1H-pyrazol-1-yl)phenyl)-4-(pyrrolidin-1-ylmethyl)benzamide (**7l**)

White solid; yield: 70.0%; m.p. 179-180 °C; <sup>1</sup>H NMR (CDCl<sub>3</sub>, 400 MHz, δ ppm): 8.79 (d, *J* = 1.6 Hz, 1H), 8.69 (s, 1H), 8.47 (dd, *J* = 4.7, 1.2 Hz, 1H), 7.97 (s, 1H), 7.88 (d, *J* = 11.8 Hz, 1H), 7.86-7.74 (m, 4H), 7.53 (dd, *J* = 8.3, 2.0 Hz, 1H), 7.39 (d, *J* = 8.1 Hz, 2H), 7.34-7.26 (m, 1H), 7.22 (d, *J* = 8.4 Hz, 1H), 3.63 (s, 2H), 2.48 (s, 4H), 2.22 (s, 3H), 1.77 (s, 4H). <sup>13</sup>C NMR (CDCl<sub>3</sub>, 100 MHz, δ ppm): 165.92, 147.76, 146.94, 143.91, 139.50, 137.80, 136.81, 133.11, 132.79, 131.71, 129.19, 128.97, 128.29, 127.71, 127.21, 123.77, 120.68, 120.23, 118.20, 60.24, 54.20, 23.49, 17.69. HRMS (ESI): *m/z* 438.2294 calcd for  $C_{27}H_{27}N_5O$  [M+H]<sup>+</sup>, found 438.2292.

4.1.5.13 4-((4-ethylpiperazin-1-yl)methyl)-N-(4-methyl-3-(4-(pyridin-3-yl)-1H-pyrazol-1-yl)phenyl)benzamide (**7m**)

White solid; yield: 82.0%; m.p. 168-170 °C; <sup>1</sup>H NMR (CDCl<sub>3</sub>, 400 MHz, δ ppm): 8.80 (d, *J* = 1.4 Hz, 1H), 8.61 (s, 1H), 8.49 (d, *J* = 4.3 Hz, 1H), 7.99 (s, 1H), 7.94 (s, 1H), 7.84 (t, *J* = 10.2 Hz, 4H), 7.61 (d, *J* = 8.1 Hz, 1H), 7.38 (t, *J* = 11.9 Hz, 2H), 7.36-7.24 (m, 2H), 3.57 (s, 2H), 2.65 (dd, *J* = 19.3, 12.1 Hz, 8H), 2.27 (s, 3H), 1.43 (s, 2H), 1.17 (t, *J* = 7.2 Hz, 3H). <sup>13</sup>C NMR (CDCl<sub>3</sub>, 100 MHz, δ ppm): 165.75, 147.74, 146.92, 142.07, 139.60, 137.84, 136.83, 133.57, 132.84, 131.79, 129.29, 129.23, 128.30, 127.71, 127.32, 123.79, 120.55, 120.27, 118.05, 62.10, 52.19, 51.75, 26.90, 17.73, 10.88. HRMS (ESI): *m/z* 481.2716 calcd for  $C_{29}H_{32}N_6O$  [M+H]<sup>+</sup>, found 481.2716.

4.1.5.14 4-((4-(hydroxymethyl)piperazin-1-yl)methyl)-N-(4-methyl-3-(4-(pyridin-3-yl)-1H-pyrazol-1-yl)phenyl)benzamide (**7n**)

White solid; yield: 70.0%; m.p. 172-175 °C; <sup>1</sup>H NMR (CDCl<sub>3</sub>, 400 MHz, δ ppm): 8.80 (d, *J* = 1.4 Hz, 1H), 8.61 (s, 1H), 8.49 (d, *J* = 4.3 Hz, 1H), 7.99 (s, 1H), 7.94 (s, 1H), 7.84 (t, *J* = 10.2 Hz, 4H), 7.61 (d, *J* = 8.1 Hz, 1H), 7.38 (t, *J* = 11.9 Hz, 2H), 7.36-7.24 (m, 2H), 3.57 (s, 2H), 2.65 (dd, *J* = 19.3, 12.1 Hz, 8H), 2.27 (s, 3H), 1.43 (s, 2H), 1.17 (t, *J* = 7.2 Hz, 3H). <sup>13</sup>C NMR (CDCl<sub>3</sub>, 100 MHz, δ ppm): 165.75, 147.74, 146.92, 142.07, 139.60, 137.84, 136.83, 133.57, 132.84, 131.79, 129.29, 129.23, 128.30, 127.71, 127.32, 123.79, 120.55, 120.27, 118.05, 62.10, 52.19, 51.75, 26.90, 17.73, 10.88. HRMS (ESI): *m/z* 497.2665 calcd for  $C_{29}H_{32}N_6O_2$  [M+H]<sup>+</sup>, found 497.2662.

4.2. BCR-ABL kinase inhibitory assay

The Kinase-Glo luminescent kinase assay is a homogeneous non-radioactive method for determining the activity of purified kinases by quantifying the amount of ATP remaining in solution following a kinase reaction. Compound **7a-7n** was dissolved in

DMSO as 5mM stock solution. Then, the stock solution was diluted to 1000 μM with DMSO and transferred to the dose plate. The compound was serially diluted with DMSO in 5-fold. Then, each concentration was diluted 10-fold with reaction buffer to obtain a 10X final concentration. The compounds were transferred with their concentrations ranging from 100 μM to 0.006 μM to an assay plate for the BCR-ABL activity test with a volume of 1 μL/well. The positive compound STSP, with a stock concentration of 10 mM in DMSO, was diluted with DMSO to 100 μM and then 5-fold serially diluted with DMSO. Each concentration in DMSO is 10-fold diluted with reaction buffer to obtain 10X final concentration. The STSP in concentrations ranging from 10 μM to 0.00064 μM was transferred to an assay plate for the BCR-ABL activity test with 1 μL/well. For HPE (no kinase and no compound, but containing ATP, substrate and 1% DMSO) and ZPE (no compound but containing kinase, ATP, substrate and 1% DMSO) well, 2 μL DMSO 10-fold was diluted with reaction buffer (containing 25 mM HEPES, 10 mM MgCl<sub>2</sub>, 100 μg/mL BSA, 0.01% TritonX-100, 2.5 mM DTT and adjusted pH to 7.4) to obtain 10% DMSO solution. It was then transferred to the assay plate at 1 μL/well. The procedure of kinase reaction is: 1) Add 10× compound to the assay plate in a 384-well plate layout, 1 μL/well. For the HPE and ZPE well, equal volume (1 μL/well) of 10% DMSO was added to the 384-well assay plate; 2) Add 2.5× kinase ABL1 into the assay plate as 384-well plate layout, 4μL/well. For HPE wells, equal volume (4 μL/well) of assay buffer was added to the 384-well assay plate; 3) Centrifuge the assay plate with 1000 rpm for 1 min to mix them; 4) Pre-incubate the assay plate at 30 °C for 30 min; 5) Mix an equal volume of 4× ATP and 4 X substrate to obtain 2× ATP-substrate mixtures. 2 X ATP-ABL tide mixture is the reaction mixture for kinase ABL1. 6) Add 2×ATP-substrate mixture to the assay plate, 5 μL /well; 7) Centrifuge the assay plate with 1000 rpm for 1 min to mix them; 8) Incubate the plate for 1 hour at 30 °C; 9) Kinase-glo was added to each well (10 μL/well), and then incubated for 20 min at 27 °C; 10) Read luminescence signal with Envision. The raw data were analyzed by Prism 5.0, and the inhibitory rate was calculated by the following formula:

$$\text{Compound inhibitory rate} = \left( \frac{\text{“compound” reading-ZPE}}{\text{HPE-ZPE}} \right) \times 100\%$$

4.3. K562 Cells growth inhibitory assay

Growth inhibitory activities were evaluated on K562 leukemia cancer cell lines. The effects of the compounds on cell viability were evaluated using the MTT assay. Exponentially growing cells were harvested and plated in 96-well plates at a concentration of  $1 \times 10^4$  cells/well, and incubated for 24 h at 37 °C. The cells in the wells were, respectively, treated with target compounds at various concentrations for 48 h. Then, 20 mL MTT (5 mg/mL) was added to each well and incubated for 4 h at 37 °C. After the supernatant was discarded, 150 mL DMSO was added to each well, and the absorbance values were determined by a microplate reader (Bio-Rad Instruments) at 490 nm. The IC<sub>50</sub> values were calculated according to inhibition ratios.

4.4. Molecular docking methods

4.4.1. BCR-ABL kinase core initial model building

The BCR-ABL kinase core model was generated by Discovery Studio 4.0 (DS4.0) based on the 3cs9 protein crystallographic structure. Unwanted water and ligands were removed by the DS4.0, and the lost atoms such as hydrogen were added to build the initial receptor structure for docking.<sup>14</sup>

4.4.2. Small molecular preparation

The structure of **7a** and **7i** was drawn by Gaussian03 software, then optimized the molecules to the minimum energy conformation used the semi-empirical AM1 method.

#### 4.4.3. Docking protocol

Docking procedure was performed by AutoDock 4 software with the help of Autodock Tools. Firstly, the no-polar hydrogen of receptor and ligands were removed, and then add the Computer Gasteiger charge for receptor and ligands. The grid maps were calculated using AutoGrid4 for three dockings, a grid map with 70×80×70 points and a grid-point spacing of 0.375 Å was applied. In order to fully explore the possible binding conformations, 100 conformations were generated using the Lamarckian Genetic Algorithm (LGA). For other docking parameters, standard values were used as software default. Cluster analysis was performed on the results using a root mean square (RMS) tolerance of 2.0 Å. The conformations and binding energy for further analysis were obtained from the average of the biggest cluster.<sup>15</sup>

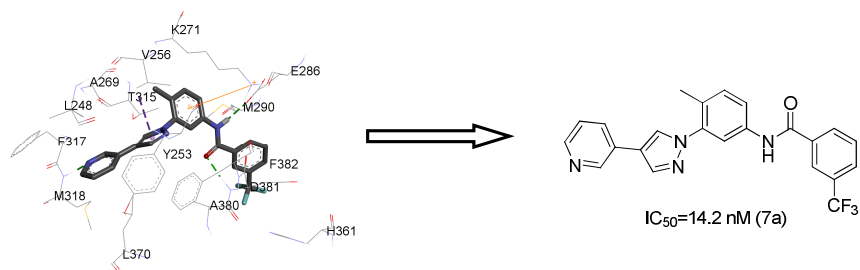
#### Acknowledgments

The authors would like to acknowledge financial support from the Chinese Natural Science Foundation Project (21272020), the Project of Construction of Innovative Teams and Teacher Career Development for Universities and Colleges Under Beijing Municipality (IDHT20140504).

#### References and notes

1. Y.P. Li; M.J. Shen; Z. Zheng; J.F. Luo; X.F. Pan; X.Y. Lu; H.Y. Long; D.H. Wen; F.X. Zhang; F. Leng; Y.J. Li; Z.C. Tu; X.M. Ren; D. Ke. *J. Med. Chem.* **2012**, 55, 10033.
2. S.X. Li; Z.L. Yao; Y.J. Zhao; W. Chen; H.J. Wang; X.Z. Kuang; W.H. Zhan; S. Yao; S.Y. Yu; W.X. Hu. *Bioorg. Med. Chem. Lett.* **2012**, 22, 5279.
3. H.J. Choe; J. Kim; S.W. Hong. *Bioorg. Med. Chem. Lett.* **2013**, 23, 4324.
4. S.M. Yun; K.H. Jung; S.J. Kim; Z.H. Fang; M.K. Son; H.H. Yan; H.S. Lee; J.H. Kim; S.H. Shin; S.W. Hong; S.S. Hong. *Cancer Lett.* **2014**, 348, 50.
5. D.B. Zhou; Y.T. Qiu; Z.C. Tu; C.Z. Liao; Q.Q. Meng; R.S. Yao; Z. Li; S. Jiang. *Sci China Chem.* **2014**, 57, 823.
6. F. Manetti; C. Brullo; M. Magnani; F. Magnani; B. Chelli; E. Crespan; S. Schenone; A. Naldini; O. Bruno; M.L. Trincavelli; G. Maga; F. Carraro; C. Martini; F. Bondavalli; M. Botta. *J. Med. Chem.* **2008**, 51, 1252.
7. M.V. Ramana Reddy; V.R. Pallela; S.C. Cosenza; M.R. Mallireddigari; R. Patti; M. Bonagura; M. Truongcao; B. Akula; S.S. Jatiani; E. Premkumar Reddy. *Bioorg. Med. Chem.* **2010**, 18, 2317.
8. X.M. Ren; X.F. Pan; Z. Zhang; D.P. Wang; X.Y. Lu; Y.P. Li; D.H. Wen; H.Y. Long; J.F. Luo; Y.B. Feng; X.X. Zhuang; F.X. Zhang; J.Q. Liu; F. Leng; X.F. Lang; Y. Bai; M.Q. She; Z.C. Tu; J.X. Pan; K. Ding. *J. Med. Chem.* **2013**, 56, 879.
9. H.G. Park; S.H. Hong; J.H. Kim; S.W. Hong. *J. Am. Chem. Soc.* **2013**, 135, 8227.
10. W.S. Huang; C.A. Metcalf; R.J. Sundaramoorthi; Y.H. Wang; Z. Dong; R.M. Thomas; X.T. Zhu; L.S. Cai; D. Wen; S.Y. Liu; J. Romero; J.W. Qi; I. Chen; G. Banda; S. P. Lentini; S. Das; Q.H. Xu; F. Wang; S. Wardwell; Y.Y. Ning; J.T. Snodgrass; M.I. Broudy; K. Russian; T.J. Zhou; L. Commodore; N.I. Narasimhan; Q.K. Mohemmad; J. Iulucci. *J. Med. Chem.* **2010**, 53, 4701.
11. M. Thomas; W.S. Huang; D. Wen; X.T. Zhu; S.Y. Liu; I. Chen; J. Romero; D. Zou; R. Sundaramoorthi; F. Li; J.W. Qi; L.S. Cai; T.J. Zhou; L. Commodore; Q.H. Xu; J. Keats; F. Wang; S. Wardwell; Y.Y. Ning; J.T. Snodgrass; M.I. Broudy; K. Russian; J. Iulucci; V.M. Rivera; T.K. Sawyer; D.C. Dalgarno; T. Clackson; W.C. Shakespeare. *Bioorg. Med. Chem. Lett.* **2011**, 21, 3743.
12. M. Mojzych; V. Subertov; A. Bielawska; K. Bielawski; V. Bazgier; K. Berka; T. Gucký; E. Fornal; V. Krystof. *E. J. Med. Chem.* **2014**, 78, 217.
13. L.F. Yang; X.M. Xu; Y.L. Huang; B. Zhang; C.C. Zeng; H.Q. He; C.X. Wang; L.M. Hu. *Bioorg. Med. Chem. Lett.*, **2010**, 20, 5496.
14. Accelrys Software Inc. Discovery Studio Modeling Environment, Release 4.0; San Diego: Accelrys Software Inc. *Eur. J. Med. Chem.* **2013**.
15. G. M. Morris; D. S. Goodsell; R. S. Halliday; R. Huey; W. E. Hart; R. K. Belew and A. J. Olson. *J. Comput. Chem.*, **1998**, 19, 1639.

## Graphical abstract



ACCEPTED MANUSCRIPT